Metabolism

Molecular Cancer Research

Prostate Tumor Cell–Derived IL1β Induces an Inflammatory Phenotype in Bone Marrow Adipocytes and Reduces Sensitivity to Docetaxel via Lipolysis-Dependent Mechanisms

Mackenzie K. Herroon[1], Jonathan D. Diedrich[1,2,5], Erandi Rajagurubandara[1], Carly Martin[1,2,5], Krishna R. Maddipati[3], Seongho Kim[2,5], Elisabeth I. Heath[2,5], James Granneman[4], and Izabela Podgorski[1,2,5]

Abstract

Adipocyte–tumor cell cross-talk is one of the critical mediators of tumor progression and an emerging facilitator of therapy evasion. Tumor cells that metastasize to adipocyte-rich bone marrow take advantage of the interplay between metabolic and inflammatory pathways to activate prosurvival mechanisms that allow them to thrive and escape therapy. Using *in vitro* and *in vivo* models of marrow adiposity, we demonstrate that metastatic prostate carcinoma cells engage bone marrow adipocytes in a functional cross-talk that promotes IL1β expression in tumor cells. Tumor-supplied IL1β contributes to adipocyte lipolysis and regulates a proinflammatory phenotype in adipocytes via upregulation of COX-2 and MCP-1. We further show that the enhanced activity of the IL1β/COX-2/MCP-1 axis and a resulting increase in PGE_2 production by adipocytes coincide with augmented hypoxia signaling and activation of prosurvival pathways in tumor cells, revealing a potential mechanism of chemoresistance. The major consequence of this interplay is the reduced response of prostate cancer cells to docetaxel, a phenomenon sensitive to the inhibition of lipolysis.

Implications: Studies presented herein highlight adipocyte lipolysis as a tumor-regulated metabolic event that engages proinflammatory cross-talk in the microenvironment to promote prostate cancer progression in bone. Understanding the impact of bone marrow adipose tissue on tumor adaptation, survival, and chemotherapy response is fundamentally important, as current treatment options for metastatic prostate cancer are palliative.

Introduction

Growing evidence suggests that tumor cells can be protected from therapy-induced cell death via signaling events driven by neighboring cells. Specifically, the aggressive and often lethal phenotype of bone trophic cancers, such as tumors of the prostate and breast, acute myeloid leukemia, or multiple myeloma, is increasingly being attributed to adipocytes, a significant component of adult bone marrow (1–3). However, understanding the molecular mechanisms driving adipocyte–tumor cell cross-talk toward progression and therapy evasion has been very limited and remains a critical gap in designing effective therapies for metastatic disease. For a patient with advanced prostate cancer, current therapeutic approaches include androgen deprivation therapy in combination with microtubule-targeting docetaxel, a first life-prolonging drug for metastatic prostate cancer, and a standard-of-care treatment since 2004 (4). Unfortunately, the majority of patients eventually progress and succumb to the disease, and overcoming chemotherapy resistance remains an unmet clinical need (5). Whether marrow adiposity is a contributing factor to this limited chemotherapy response is not well understood.

It is becoming increasingly evident that the metastatic tumor cells colonizing bone marrow modulate the metabolic phenotype of marrow fat cells, thereby supporting tumor progression (6–8). Specifically, prostate carcinoma cells can stimulate triglyceride hydrolysis (lipolysis) in marrow adipocytes (7), a phenomenon also observed in adipocytes interacting with breast, ovarian, and colon cancer cells, as well as leukemic blasts (1). In return, adipocyte-supplied fatty acids have been shown to fuel the metabolism of the cancer cell and ultimately promote tumor growth and survival (1, 7, 9, 10). In addition to fatty acids, the repertoire of factors supplied by marrow fat cells includes hormones, adipokines, cytokines, incretins, growth factors, and bioactive lipids

[1]Department of Pharmacology, Wayne State University School of Medicine, Detroit, Michigan. [2]Department of Oncology, Wayne State University School of Medicine, Detroit, Michigan. [3]Department of Pathology, Wayne State University School of Medicine, Detroit, Michigan. [4]Center for Molecular Medicine and Genetics, Wayne State University School of Medicine, Detroit, Michigan. [5]Karmanos Cancer Institute, Detroit, Michigan.

Note: Supplementary data for this article are available at Molecular Cancer Research Online (http://mcr.aacrjournals.org/).

M.K. Herroon and J.D. Diedrich contributed equally to this article.

Corresponding Author: Izabela Podgorski, Wayne State University School of Medicine, 540 E. Canfield, Room 6304, Detroit, MI 48201. Phone: 313-577-0514; Fax: 313-577-6739; E-mail: ipodgors@med.wayne.edu

Mol Cancer Res 2019;17:2508–21

doi: 10.1158/1541-7786.MCR-19-0540

mediators (2, 11, 12). These molecules contribute to a number of key processes including regulation of inflammation, insulin sensitivity, and redox metabolism, and are subject to modulation by the metabolic events within the fat cell as well as cues from the microenvironment (2, 11).

Activation of lipolysis (13) or exposure to a hypoxic microenvironment (14) are examples of metabolic and environmental cues associated with adipose tissue inflammation, increased expression of cyclooxygenase-2 (COX-2), and augmented biosynthesis of prostaglandins by white adipose tissue. Both hypoxia and lipolysis also contribute to the increased production of proinflammatory factors such as macrophage chemoattractant protein (MCP-1; CCL2) or interleukin-6 (IL6; refs. 13, 15). COX-2 and MCP-1 play critical functions in the regulation of bone homeostasis and prostate cancer progression (2, 16), yet their involvement in tumor cell–adipocyte cross-talk in metastatic prostate cancer has not been investigated.

In addition to hypoxia or lipolytic stimulation, expression of proinflammatory genes such as COX-2 or MCP-1 can be modulated by other proinflammatory molecules supplied by neighboring cells, including tumor necrosis factor α (TNFα) or interleukin 1β (IL1β; refs. 17–19). Specifically, tumor cell–derived IL1β has been shown to induce COX-2 levels in tumor-associated mesenchymal stem cells leading to skeletal progression of prostate PC3-ML tumors (20). This is of significance, as we have previously shown that IL1β expression is highly induced in experimental prostate cancer bone tumors from mice with diet-induced marrow adiposity, and its secretion is augmented in tumor cells exposed to adipocyte-conditioned media (21). Other studies have reported augmented IL1β expression in metastatic prostate cancer as compared with primary tumors (20) and IL1β presence in the tumor was demonstrated to be important for seeding in the skeletal niche (22). The potential role of tumor-supplied IL1β in regulating inflammatory pathways in bone marrow adipose tissue and its effects on response to chemotherapy have not been previously addressed.

The goal of the present study was to investigate the molecular mechanisms driving a cross-talk between prostate cancer cells and bone marrow adipocytes in the context of tumor survival and therapeutic response. Using three different *in vivo* models of marrow adiposity, as well as *in vitro* coculture systems, we demonstrate that exposure to marrow adipocytes significantly augments IL1β levels in metastatic tumor cells. We also show that tumor cell–derived IL1β induces the adipocyte expression of COX-2 and microsomal prostaglandin E synthase (mPGES), two enzymes involved in the biosynthesis of prostaglandin E_2 (PGE_2). This apparent tumor-induced adipocyte inflammation is further exhibited by augmented expression of MCP-1. We show that both tumor IL1β levels and adipocyte COX-2/MCP-1 expression are induced by the stimulation of lipolysis. We also demonstrate that sensitivity of prostate cancer cells to docetaxel treatment is enhanced both by siRNA-mediated silencing of IL1β and pharmacologic inhibition of lipolysis. Our studies point to PGE_2 supplied by adipocytes as a potential regulator of prosurvival pathways in the tumor. These findings are first to demonstrate the interaction between tumor-supplied IL1β and marrow adipocyte COX-2/MCP-1 pathways, and offer important insight into the potential involvement of this cross-talk in therapeutic response in metastatic disease.

Materials and Methods

Materials

DMEM, RPMI-1640, insulin, and isoproterenol were obtained from Sigma-Aldrich. HyClone FBS, TRIzol, TaqMan reagents, and RNAiMAX were from Thermo Fisher Scientific. Trypsin-EDTA and collagenase were from Invitrogen. PureCol collagen type I was from Advanced Biomatrix. Transwell cell-support systems were from Corning. Z-fix was from Anatech Ltd. StemXVivo Adipogenic Supplement, Cultrex, recombinant IL1β, and recombinant IL1RA were from R&D Systems. β-Tubulin (#E7-C) antibody was from Developmental Studies Hybridoma Bank. β-Actin antibody (#NB600-501) was from Novus Biologicals. Antibodies to IL1β (#12703), Cyclin D (#2978), p-GSK-3β (#5558), GSK-3β (#12456), and p-β-Catenin (#9561) were from Cell Signaling Technology. Cyclooxygenase 2 (COX-2; #ab15191) antibody was from Abcam. β-Catenin antibody (#610153) was from BD Transduction Laboratories. RNeasy Mini Kits were from Qiagen. Immunoblotting Luminata Forte Western HRP substrate was from EMD Millipore. Rosiglitazone, CAY10585, BAY 11-7082, and Forskolin were from Cayman Chemical. BAY59-9435 was a kind gift from Dr. Young-Hoon Ahn (WSU). ImmPACT NovaRED Peroxidase Substrate and ImmPRESS Anti-Rabbit Peroxidase Reagent kit were from Vector Laboratories.

Cell lines

PC3 cells were purchased from ATCC. ARCaP(M) cells were purchased from Novicure Biotechnology. Murine RM-1 cell line was a kind gift from Dr. Timothy Thompson (MD Anderson, Houston, TX). PC3 and RM-1 cells were cultured in DMEM with 10% FBS, and ARCaP(M) cells were cultured in RPMI-1640 with 5% FBS. All media were supplemented with 10 mmol/L HEPES, and 100 U/mL penicillin–streptomycin. Primary mouse bone marrow stromal cells (mBMSC) were isolated from tibiae and femurs of 6- to 8-week-old FVB/N mice. To induce bone marrow adipocyte differentiation, mBMSCs were treated with adipogenic cocktail (30% StemXVivo Adipogenic Supplement, 1 μmol/L insulin, 2 μmol/L Rosiglitazone) for 8 to 10 days as previously described (21). Human cell lines used in this study have been authenticated by the WSU Genomics facility. All cell lines are routinely tested for *Mycoplasma* using MycoFluor Mycoplasma Detection Kit (Thermo Fisher) and LookOut Mycoplasma PCR Detection Kit (Sigma). Cells are used within 10 to 12 passages from thawing. All cells are maintained in a 37°C humidified incubator ventilated with 5% CO_2.

Clinical specimens

Bone biopsy tissue specimens were obtained from prostate cancer patients enrolled in human protocol #2011-185 and approved by the Karmanos Cancer Institute and Wayne State University Institutional Review Board. Written informed consent was obtained from all patients participating in the study, and all IHC analyses were performed according to procedures approved by the protocol and in agreement with protocol guidelines and regulations.

Animals

All experiments involving mice were performed in accordance with the protocol approved by the institutional Animal Investigational Committee of Wayne State University and NIH

guidelines. *In vivo* xenograft studies and subcutaneous tumors using either low-fat (LFD), high-fat (HFD), or Rosiglitazone (ROSI) diet were performed in 8- to 10-week-old male mice in the FVB/N background with homozygous null mutation in the Rag-1 gene (FVB/N/Rag-$1^{-/-}$), bred in house. *In vivo* syngeneic studies in genetically obese mice were performed in 3-month-old male mice with the homozygous *Lep*^{ob} mutation (ob/ob) in C57BL/6J background (Jackson Laboratory). C57BL/6J mice were used as control group.

Diets

At 5 weeks of age, FVB/N/Rag-$1^{-/-}$ mice were started on LFD (10% calories from fat; Research Diets D12450Ji), HFD (60% calories from fat; Research Diets D12492i), or 20 mg/kg ROSI diet (Research Diets D15022201i; 10% calories from fat supplemented with Rosiglitazone from Cayman Chemical by Research Diets). D12450Ji is a standard matched control diet used for both D12492i and D15022201i (as recommended by Research Diets). Mice were maintained on diets for 8 weeks (LFD/HFD) or 14 weeks (LFD/ROSI) prior to tumor implantation and continued on the respective diets after implantation. Diet and water were available *ad libitum*.

Intratibial and subcutaneous injection of prostate cancer cells

Intratibial and subcutaneous tumor injections were performed under isoflurane inhalation anesthesia according to our published procedures (7, 21). Mice were euthanized 2 weeks (RM-1 cells), 6 weeks (PC3 cells), or 8 weeks (ARCaP(M) cells) after injection. X-ray images of tumor-bearing and control bones were obtained using a Carestream *In Vivo* Xtreme Imager. Tibiae samples and subcutaneous tumors were fixed either in Z-fix, decalcified, and embedded in paraffin for tissue staining, or snap-frozen in liquid nitrogen, powderized, and stored at −80°C for RNA and lipidomic analyses. RNA was extracted using TRIzol, chloroform, and alcohol, followed by the protocol from RNeasy Mini Kit.

Quantification of adipocyte numbers and IHC

Longitudinal sections (5 μm thick) from the control and tumor-bearing tibiae were deparaffinized and stained with H&E as described previously (21). Digital images were captured under 4× magnification using an Olympus BX43 upright light microscope with UC50 (CCD chip) camera (Olympus Scientific Solutions). The entire area of each tibia was reconstructed from the 4× images. To quantify adipocytes, the marrow of the bone from the growth plate to the tibiofibular junction was outlined in ImageJ and the adipocytes within the region were manually counted using ImageJ Cell Counter function. For IHC analyses of IL1β expression, ImmPRESS Anti-Goat Peroxidase Polymer Detection systems along with a NovaRED kit as a substrate were used for the peroxidase-mediated immunostaining reaction.

Transwell cocultures and conditioned media treatments

Two-dimensional (2D) Transwell cocultures with adipocytes were performed according to our established protocols (7, 23). All experiments were performed at either normoxic (21% O_2; 5% CO_2) or hypoxic (1% O_2; 5% CO_2) condition as specified. HIF1α inhibitor CAY10585 (5 μmol/L) treatments were applied overnight prior to sample collection. Forskolin (20 μmol/L), Isoproterenol (10 μmol/L), BAY59-9435 (5 μmol/L), recombinant human IL1β (5 ng/mL), and recombinant human IL1RA (200 ng/mL) treatments were applied upon seeding. Conditioned media from PC3 and ARCaP(M) cells were generated from 48 hours in 100 mm and used to treat adipocytes at 1:1 with serum-free media (SFM) for 48 hours. RNA from tumor cells and adipocytes was extracted using RNeasy Plus Mini Kit. For protein collection, cells were washed with PBS and collected using SME (prostate cancer cells) or RIPA buffer (adipocyte cells) containing protease (MBL International) and phosphatase (Thermo Fisher Scientific) inhibitors. For ELISA assays, Transwell cultures were washed with PBS and changed to SFM overnight. Media were collected, spun down, snap frozen, and stored at −80°C. ELISA assay was performed according to the manufacturer's protocol (R&D Systems).

For three-dimensional (3D) Transwell cocultures, adipocytes were prepared in collagen gels as described for the 2D system (7, 21, 23). 3D cultures of ARCaP(M) and PC3 cells were established on coverslips as described previously (24). Briefly, single-cell suspensions containing 10,000 cells were plated on top of coverslips coated with Cultrex. One 3D coverslip was then placed on each Transwell membrane positioned above differentiated adipocyte culture and overlaid with 2% Cultrex in growth media allowing for free exchange of nutrients between the compartments. Cultures were established for 48 hours and exposed to siRNA approaches and docetaxel treatment as indicated.

Lipidomic analyses

PC3 and ARCaP(M) cells were grown alone or in Transwell coculture with marrow adipocytes for 48 hours, washed with PBS, and changed to SFM overnight. Culture supernatants and tumor cell pellets were collected separately, snap-frozen, and stored at −80°C. Control and tumor-bearing tibiae from LFD and HFD mice were snap-frozen, powderized, resuspended in methanol at a protein concentration of 200 mg/mL, and stored at −80°C until use.

Fatty acyl lipidomic analysis of media samples and bone extracts was performed by LC-MS as described earlier with minor modifications (13, 25). Briefly, the samples were spiked with a mixture of deuterated internal standards (PGE_1-d4, RvD2-d5, LTB_4-d4, 15-HETE-d8, and 14(15)-EpETrE-d11) for quantitation and purified by solid phase extraction using C18 cartridges (StrataX C18, 30 mg, Phenomenex). The extracts were directly analyzed by LC-MS using optimized Multiple Reaction Monitoring methods and each peak detected was further analyzed by Enhanced Product Ion mass spectrum for confirmation (QTRAP5500, Sciex). LC-MS data were analyzed by MultiQuant (Sciex), and relative quantitation was performed against internal standards. MarkerView (a multivariate analysis software to analyze the mass spectral data by ABSCIEX) was performed to identify compounds that significantly differ between samples. For lipids extracted from media samples, changes in eicosanoid levels between the sum (T + A) of single cultures of tumor cells (T) and adipocytes (A) and the Transwell coculture (AT) were determined. For the *in vivo* samples, changes in eicosanoid levels between control and tumor-bearing bone for each diet were determined. Significantly changed lipids were found using volcano plots based on unadjusted $P \leq 0.05$ and fold change ≥ 1.5.

Immunoblot analyses

Lysate samples were loaded based on DNA concentrations and proteins were electrophoresed on 12% or 15% SDS-PAGE gels,

transferred to PVDF membranes (Bio-Rad), and immunoblotted for indicated proteins, using peroxidase-labeled secondary antibodies. All images comply with the digital image and integrity policies. Densitometry using FujiFilm's (Minato) Multi Gauge software was used to verify the fold change in protein levels between conditions.

TaqMan RT-PCR

The cDNA from cells and *in vivo* samples was prepared using High-Capacity cDNA Reverse Transcription kit (Thermo Fisher Scientific). The analyses of genes were performed using TaqMan Individual Gene-Expression assays for Human *IL1β* (Hs00174097), *COX-2* (PTGS2; Hs00153133), *mPGES* (PTGES; Hs00610420), *MCP-1* (CCL2; Hs00234140), Murine *IL1β* (Mm00434228), *COX-2* (Mm03294838), *mPGES* (PTGES; Mm00452105), *GLUT1* (SLC2A1; Mm00441480), *HIF1α* (Mm00468869), and *MCP-1* (CCL2; Mm00441242). Assays were done on three biological replicates using TaqMan Fast Universal PCR Master Mix and 50 ng of cDNA/well. All reactions were run on an Applied Biosystems StepOnePlus system, and data were normalized to *hypoxanthine phosphoribosyltransferase* (HPRT1; Hs02800695), *18S* (Hs03003631), or *adiponectin* (Adipoq; Mm00456425). DataAssist Software (Thermo Fisher Scientific) was used for all analyses.

NFkB/p65 immunocytochemistry

Adipocytes were cultured alone, in the presence of recombinant human IL1β (for 4 hours) or in Transwell coculture with ARCaP(M) cells (for 24 hours). Where specified, NFκB inhibitor (BAY 11-7082) was added at plating. Adipocyte cultures were fixed with 3.7% formaldehyde, stained with NFκB (p65) antibody (Cell Signaling Technology; #8242), and imaged on a Zeiss LSM 780 confocal microscope with a 40× water immersion objective.

siRNA approaches

For gene-expression analyses, PC3 or ARCaP(M) cells were plated in 6-well plates or on Transwell filters and grown overnight, then a unique 27mer siRNA duplex targeting IL1β transcripts (OriGene: SR302365, Locus ID 3553) or Trilencer-27 Universal scrambled negative control (Origene: SR30004) was added using RNAiMAX transfection reagent at a final concentration of 20 μmol/L (based on the manufacturer's protocol). After 6 hours to overnight, cells were moved into Transwell coculture with adipocytes or grown alone. After 48 hours, cells were collected and processed for RNA analyses as described above. For Live/Dead assays, 3D cultures were treated with IL1β siRNA duplex or scrambled control and exposed to docetaxel 24 hours later as described below.

Live/Dead assays in 3D cultures

Assays were performed on live PC3 and ARCaP(M) cells using Molecular Probes Live/Dead Viability/Cytotoxicity Kit (Invitrogen). Clinical-grade docetaxel (DCTx) was a kind gift from Karmanos Cancer Institute Pharmacy. Established 3D spheroids were treated with either DCTx (10 nmol/L) or vehicle (1% ETOH) for 72 hours and retreated after 48 hours. For IL1β siRNA experiments, DCTx or vehicle treatments were performed for 96 hours without retreatment. For all experiments, coverslips were stained with 2 μmol/L Calcein AM and 5 μmol/L Ethidium homodimer-1 (Live/Dead Viability/Cytotoxicity Kit) for 30 minutes at room temperature, placed in PBS and immediately imaged by capturing z-stacks through the depth of structures using a Zeiss LSM 780 confocal microscope with a 40× water immersion objective. Tile images were obtained using a 10× water immersion objective. Live cells (green; Calcein AM) were captured using excitation at 488 nm and emission at 507 nm. Dead cells (red; Ethidium homodimer-1) were recorded using excitation at 488 nm, emission at 730 nm. 3D reconstruction and the sum of channel intensity were quantified using Volocity Software (PerkinElmer). For each spheroid, the volume of live signal over total signal, and dead signal over total signal, was obtained and shown as percent control of untreated cells.

In silico oncomine analyses

The Oncomine database (Oncomine v4.5: 729 data sets, 91,866 samples) was used for the analysis of primary (P) vs. metastatic (M) tumors by using filters for selection of conditions and genes of interest (prostate cancer; metastasis vs. primary; genes). Data were ordered by "overexpression" and the threshold was adjusted to $P<1E-4$; fold change, 2; and gene rank, top 10%. For each database, only genes that met the criteria for significance were reported.

Statistical analyses

An unpaired two-sided *t* test was used to compare between two groups and, for three or more groups, a one-way analysis of variance (ANOVA) was used at a 5% significance level. Data were presented as mean ± standard deviation (SD).

Results

Exposure to adipocytes reduces sensitivity of prostate cancer cells to docetaxel treatment

Previous findings from our laboratory and data by others have shown that tumor cells interacting with adipocytes are capable of taking up and utilizing adipocyte-derived lipids (1, 8, 10, 21). Specifically, transfer of lipids between fat cells and tumor cells coincides with increased tumor cell proliferation and invasiveness (10, 21), accelerated progression in bone (21), as well as changes in tumor metabolism and survival (1, 7, 8, 23). To determine whether these adipocyte-driven events might affect tumor response to therapy, we cultured ARCaP(M) 3D spheroids alone or in Transwell with adipocytes in the absence or presence of 10 nmol/L DCTx (Fig. 1). The volume of the spheroids cultured in the presence of adipocytes was visibly larger than the spheroids cultured alone, a result in agreement with our previous reports of growth-promoting effects of adipocytes (ref. 24; Fig. 1A and B, vehicle). Strikingly, this difference in spheroid size between Transwell and control cultures persisted throughout the 5-day treatment with 10 nmol/L DCTx (Fig. 1A and B, DCTx). Furthermore, ethidium homodimer-1 staining (Live/dead assay) demonstrated that the number of dying ARCaP(M) cells (Fig. 1C and D) and PC3 cells (Fig. 1E) upon DCTx treatment was reduced under Transwell conditions, indicating potential chemoprotective effects of adipocytes.

Prostaglandin synthesis is increased in marrow adipocytes interacting with prostate cancer cells *in vitro* and *in vivo*

To determine if there are specific lipid mediators responsible for protumor effects of adipocytes, we performed analyses of fatty acyl lipids present in the supernatants from marrow adipocytes and prostate cancer cells interacting via Transwell coculture

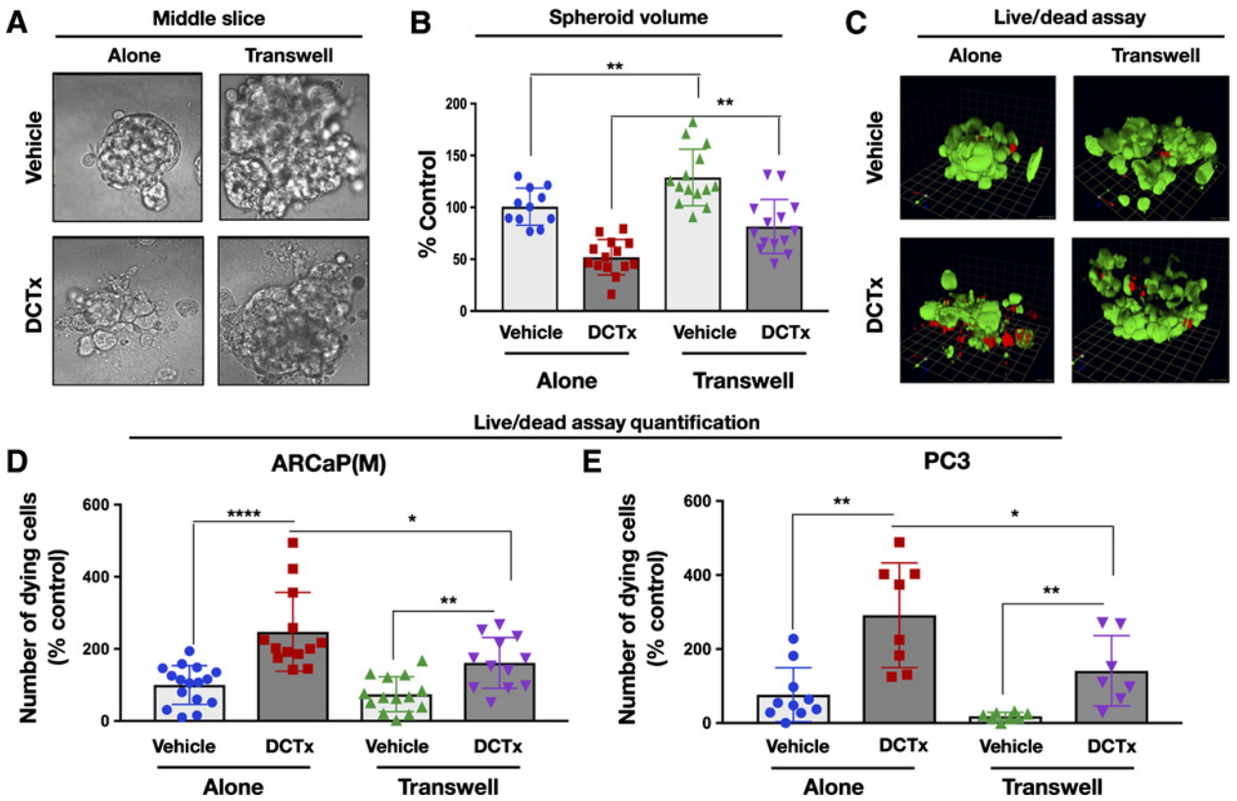

Figure 1.

Interaction with adipocytes reduces sensitivity of 3D spheroids from ARCaP(M) and PC3 cells to docetaxel (DCTx). 3D cultures of ARCaP(M) grown in Transwell coculture with bone marrow adipocytes in the absence or presence of 10 nmol/L DCTx. **A,** DIC images of a slice through the middle of 3D spheroid; **B,** Quantification of total spheroid volume; **C,** 3D reconstruction of Live/Dead assay results from ARCaP(M) spheroids grown alone or in Transwell with marrow adipocytes and treated with vehicle (EtOH) or 10 nmol/L DCTx; green: Calcein AM–positive live cells; red: ethidium homodimer–positive dead cells; Quantification of ethidium–positive (dead) ARCaP(M) cells (**D**) and PC3 cells (**E**) per total spheroid volume shown as percent control; *, $P < 0.05$; **, $P < 0.01$; ****, $P < 0.0001$.

in vitro. LC-MS/MS of nearly 200 species generated by three major pathways (cyclooxygenase, lipoxygenase, and epoxygenase) revealed that prostaglandins, products of cyclooxygenases, are the predominant lipid mediators induced in Transwell cocultures, with PGE_2, an important regulator of prosurvival pathways in the tumor (26), being the most highly augmented species (Fig. 2A and B; Supplementary Fig. S1A). This increase in prostaglandin levels was accompanied by an induced expression of prostaglandin-producing enzymes, *COX-2* and *mPGES* in adipocytes (Fig. 2C–H), but not the tumor cells (Supplementary Fig. S1B and S1C). In addition, the relative levels of the primary producer of PGE_2, *COX-2* enzyme, were significantly lower in tumor cells as compared with adipocytes (Supplementary Fig. S1D), suggesting that prostate cancer cells may not be a significant supplier of PGE_2. Notably, *COX-2* and *mPGES* expression in marrow adipocytes was not only induced by Transwell coculture with prostate cancer cells but also by tumor cell–conditioned media (Fig. 2I–L), suggesting the involvement of tumor-supplied factor in this process.

To determine whether similar effects on prostaglandin production can be driven by increased marrow adiposity *in vivo*, we examined the fatty acyl lipidome of control and tumor-bearing tibiae from mice fed LFD versus HFD, which we and others have shown to augment marrow adiposity (2, 21, 27). Mirroring our *in vitro* findings, our results revealed that PGE_2 and several other metabolites of the cyclooxygenase pathway are significantly induced in tumor-bearing bones as compared with control bones, especially in mice fed HFD (Fig. 2M; Supplementary Fig. S1F). Using human (tumor) and mouse (host)-specific TaqMan probes, we determined that augmented PGE_2 levels coincide with increased expression of host (mouse) *COX-2* (Fig. 2N) and *mPGES* (Fig. 2O) in tumor-bearing tibiae relative to control bones. Notably, the increase in the expression of host *COX-2*, the major PGE2-producing enzyme, was significantly higher in tumor-bearing tibiae of HFD mice as compared with LFD mice, whereas human *COX-2* and *mPGES* levels were not increased (Supplementary Fig. S1G and S1H). There was no cross-reactivity between the human and mouse TaqMan probes (Supplementary Fig. S1I), which further indicated that diet-induced adiposity might be increasing PGE_2 production by the host microenvironment in response to tumor. To determine if these effects are mediated by marrow adiposity rather than HFD, we evaluated the host expression of *COX-2* and *mPGES* in two other models with augmented levels of marrow fat cells: mice fed ROSI diet (28, 29) and genetically obese (ob/ob) mice (30). Both ROSI and ob/ob mice exhibited high levels of bone marrow adiposity compared with control mice (Supplementary Fig. S2A, S2B, S2F and S2G) and showed increases in *COX-2* and *mPGES* levels in tumor-bearing tibiae (Supplementary Fig. S2D, S2E, S2I and S2J),

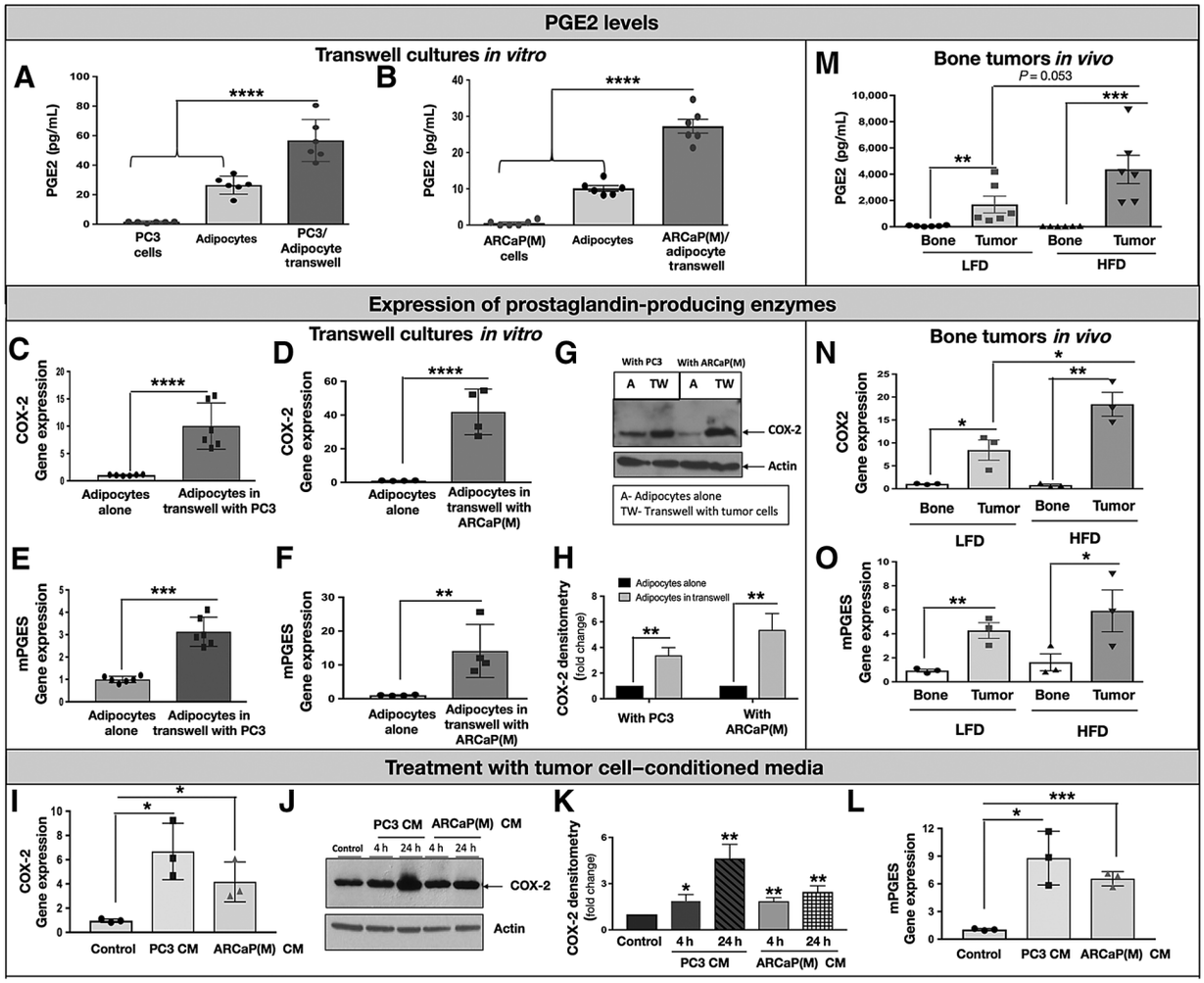

Figure 2.

Interaction with prostate cancer cells induces COX-2 signaling in adipocytes. PGE_2 levels in adipocyte cultures with PC3 (**A**) and ARCaP(M) cells (**B**) as determined by MS/MS analysis of cell culture supernatants from tumor cells alone, adipocytes alone, and Transwell cocultures. Data are from 6 replicate wells and expressed in pg/mL. TaqMan RT PCR results showing augmented *COX-2* (**C** and **D)** and *mPGES* (**E** and **F**) levels in bone marrow adipocytes cultured in Transwell with PC3 and ARCaP(M) cells; **G,** Immunoblot analysis of COX-2 protein expression levels in adipocytes cultured alone or in Transwell with PC3 and ARCaP(M) cells. **H,** Densitometric analysis of COX-2 bands normalized to Actin. Data are mean of three separate experiments. **I,** *COX-2* gene expression in adipocytes cultured alone (control) or in the presence of media conditioned by PC3 or ARCaP(M) cells (PC3 CM and ARCaP(M) CM). **J,** Immunoblot analysis of COX-2 (1:500) expression in adipocytes treated with PC3 CM and ARCaP(M) CM for 24 and 48 hours. **K,** Densitometric analysis of COX-2 bands normalized to Actin (1:1,000). Data are mean of three separate experiments. **L,** *mPGES* gene expression in adipocytes cultured alone (control) or in the presence of PC3 CM and ARCaP(M) CM. **M,** PGE_2 levels in control and tumor-bearing tibiae from LFD and HFD mice. mRNA levels of *COX-2* (**N**) and *mPGES* (**O**) in control and tumor-bearing bones as determined by TaqMan RT-PCR. *, $P < 0.05$; **, $P < 0.01$; ***, $P < 0.001$; ****, $P < 0.0001$.

suggesting adipocyte- rather than diet-mediated effects. In both ROSI and ob/ob models, bone-tumor burden was increased with augmented marrow adiposity (Supplementary Fig. S2C and S2H), similar to results previously observed with an HFD model (21). Furthermore, in line with previous reports linking *COX-2* activity with adipocyte inflammation (13), we observed highly augmented levels of *CCL2/MCP-1* cytokine in adipocytes interacting with prostate cancer cells *in vitro* and *in vivo* (Supplementary Fig. S3). Notably, in contrast to robust effects of marrow adiposity on *COX-2*, *mPGES*, and *MCP-1* levels in bone tumors, no significant differences were observed in subcutaneous tumors with diet or Rosiglitazone-mediated adiposity, suggesting this might be a bone tumor-specific phenotype (Supplementary Fig. S4).

COX-2/MCP-1 expression in marrow adipocytes is mediated by tumor cell–supplied IL1β

Both *MCP-1* and *COX-2* levels and activity can be regulated via proinflammatory processes, including IL1β-mediated activation of the IL1 receptor (IL1R; refs. 17, 31, 32). Notably, our previous studies reported *IL1β* as one of the top genes upregulated in prostate bone tumors from HFD mice (21). To examine whether this is also true for IL1β protein, we performed IHC analyses of ARCaP(M) bone tumors from LFD and HFD mice and observed strong IL1β localization to the tumor cells, along with augmented expression in tumors from mice with HFD-induced marrow adiposity (Supplementary Fig. S5A and S5B). Importantly, the presence of IL1β at the protein (Supplementary Fig. S5C)

and mRNA (Supplementary Fig. S5D) levels was also revealed in bone lesions from metastatic prostate cancer patients. This is in line with previous reports of *IL1β* expression in metastatic prostate cancer (20) and its importance for seeding in the skeletal niche (22).

To directly examine the effects of tumor cell–supplied IL1β on marrow adipocytes, we first established that expression levels and secretion of IL1β by PC3 and ARCaP(M) cells are indeed augmented at the mRNA and protein levels upon Transwell cocultures with fat cells (Fig. 3A–F). We then observed that exposure of Transwell cultures to IL1 receptor antagonist (IL1RA), or coculture with tumor cells in which IL1β expression was silenced by three nonoverlapping siRNAs, partially reduces expression of COX-2 (Fig. 3G–J), as well as *mPGES* (Fig. 3K and L) and *MCP-1* (Supplementary Fig. S6A). Reciprocally, adipocyte treatment with recombinant IL1β strongly induced *COX-2* (Fig. 3M) as well as *mPGES* (Fig. 3N) and *MCP-1* levels (Supplementary Fig. S6B), indicating IL1β-mediated effects. This IL1β-induced inflammatory phenotype appeared to be NFkB driven, as demonstrated by the nuclear localization of p65 upon IL1β treatment or exposure to Transwell adipocyte cocultures, a phenomenon reversed by the treatment with the NFkB inhibitor BAY 11-0782 (Fig. 3O and P).

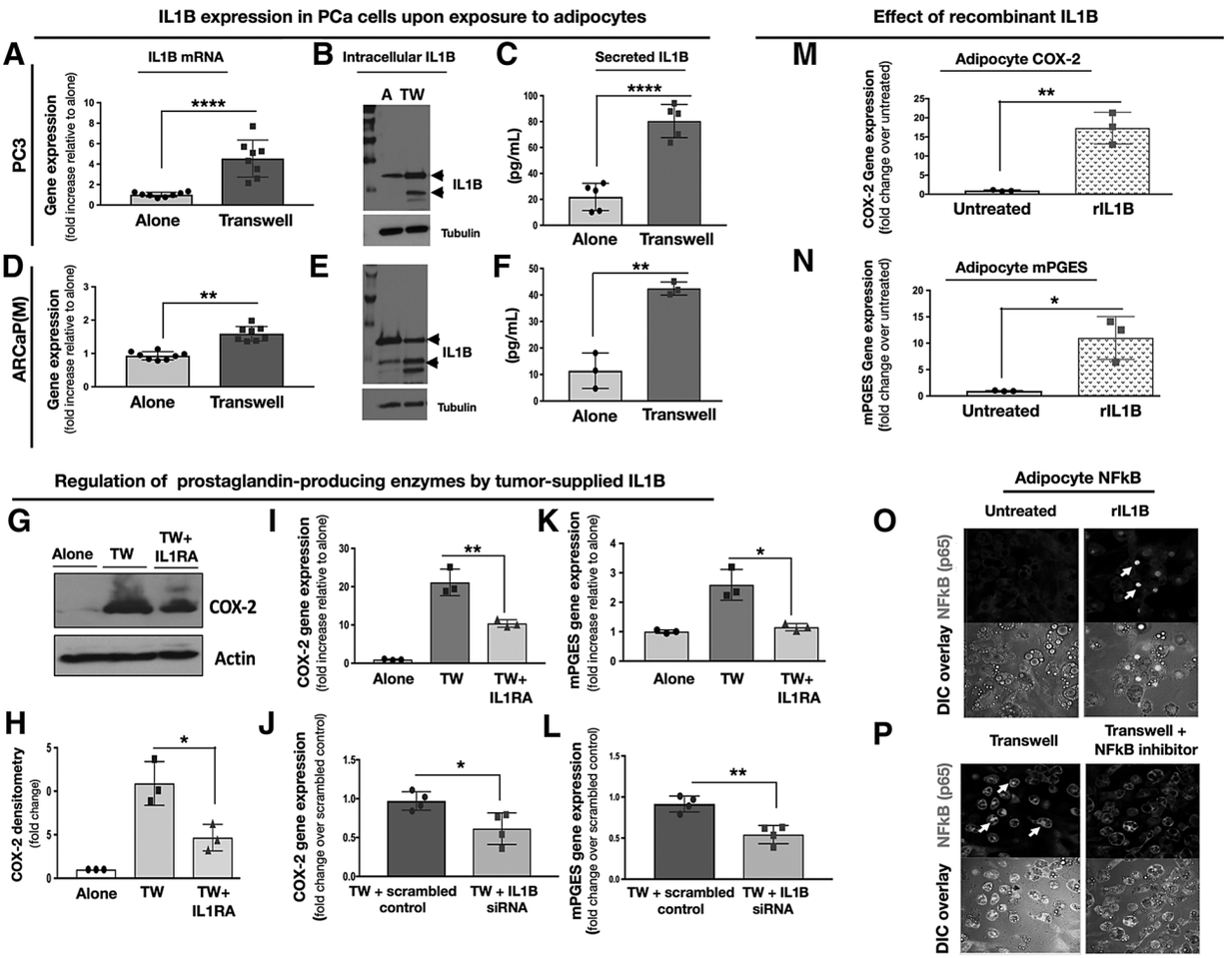

Figure 3.

Adipocyte–tumor cell cross-talk: IL1β expression and secretion by prostate carcinoma cells augments COX-2 signaling in adipocytes. PC3 (**A–C**) and ARCaP(M) cells (**D–F**) were grown alone or in Transwell coculture with bone marrow adipocytes. TaqMan RT-PCR results show highly induced mRNA levels of *IL1β* in PC3 (**A**) and ARCaP(M) cells (**D**); graph representative of multiple experiments. Immunoblot analyses depicting increased levels of IL1β (1:1,000) protein in PC3 (**B**) and ARCaP(M) cells (**E**). Tubulin (1:2000) shown for equal loading control. **C** and **F,** ELISA assay results depicting levels of IL1β secreted by PC3 cells (**C**) or ARCaP(M) cells (**F**) grown alone or in Transwell with adipocytes. **G,** COX-2 protein levels in the absence or presence of recombinant IL1RA (200 ng/mL). **H,** Densitometry of COX-2 bands normalized to actin bands; data represent the mean of three experiments **I,** *COX-2* gene expression in bone marrow adipocytes grown alone or in Transwell with ARCaP(M) cells in the absence or presence of IL1RA; **J,** siRNA-mediated IL1β knockdown in ARCaP(M) cells reduces *COX-2* gene-expression levels in marrow adipocytes grown in Transwell cultures with ARCaP(M) cells as compared with cells transfected with scrambled control; **K,** *mPGES* mRNA levels in marrow adipocytes treated with IL1RA; **L,** *mPGES* gene expression in adipocytes upon siRNA-mediated knockdown of IL1β in tumor cells; mRNA levels of *COX-2* (**M**) and *mPEGS* (**N**) in marrow adipocytes treated with recombinant IL1β. **O,** p65(NFκB) immunofluorescence in bone marrow adipocytes grown under control conditions or treated with recombinant IL1β. NFκB activation is demonstrated by the nuclear p65 staining in response to IL1β. **P,** Marrow adipocytes grown in Transwell with ARCaP(M) cells. Reduced nuclear p65 upon treatment with NFκB inhibitor BAY 11-0782. *, $P < 0.05$; **, $P < 0.01$; ****, $P < 0.0001$.

IL1β/COX-2/MCP-1 cross-talk is stimulated by lipolysis

Previous studies in white adipose tissue showed that COX-2 and MCP-1 expression in fat cells is sensitive to stimulation of lipolysis (13). Our previous work has also shown that Transwell coculture of adipocytes with prostate cancer cells leads to the release of free glycerol, indicating activation of lipolysis. This process was reversed by the inhibition of adipocyte triglyceride lipase (ATGL), suggesting tumor contribution to the regulation of lipolytic machinery in fat cells (7). Intriguingly, treatment with lipolysis-promoting agents, such as Isoproterenol (Fig. 4A–C) or Forskolin (Fig. 4D–F), significantly increased IL1β expression already augmented by adipocytes in Transwell cultures. Reciprocally, treatment with BAY59-9435, an inhibitor of hormone-sensitive lipase (HSL), significantly reduced *IL1β* levels (Fig. 4G). Similar modulatory effects of lipolysis were observed for *COX-2*, *mPGES*, and *MCP-1* whose levels were significantly increased by Forskolin (Fig. 4H; Supplementary Fig. S6C and S6D, left) and reduced by BAY59-9435 (Fig. 4I; Supplementary Fig. S6C and S6D, right). Interestingly, treatment of adipocytes with recombinant IL1β induced the expression of *HSL* and *ATGL*, as well as the release of free glycerol (Fig. 4J and K), underscoring the potential contribution of tumor-supplied IL1β to the inflammatory phenotype in adipocytes and suggesting lipolysis might be involved in regulation of tumor cell–adipocyte cross-talk.

Sensitivity of prostate carcinoma cells to DCTx treatment is regulated by IL1β and lipolysis

Given the strong IL1β presence in metastatic tissues from prostate cancer patients, and its regulation by marrow adipocytes, we wondered whether the reduced sensitivity to DCTx in the

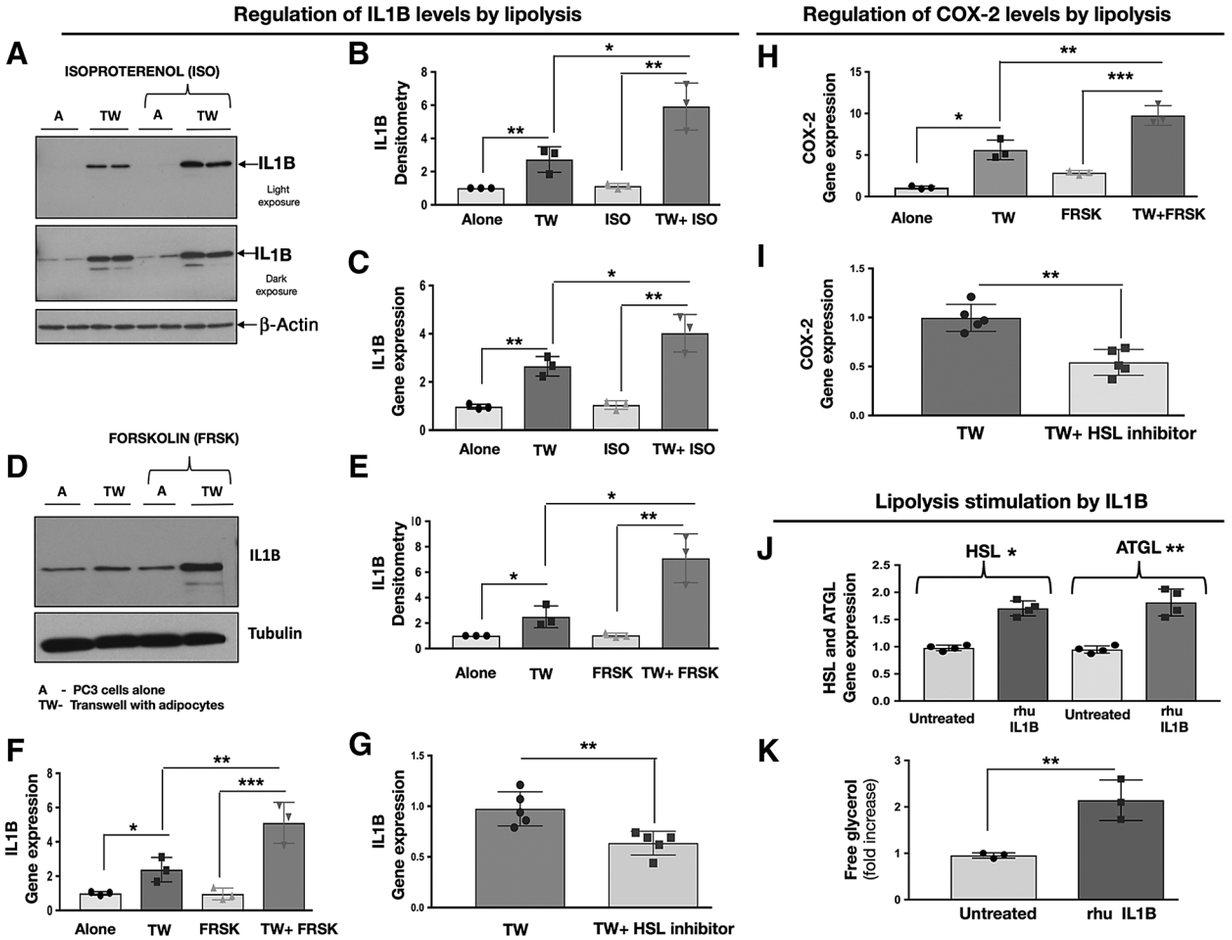

Figure 4.

IL1β expression in PC3 cells and COX-2 levels in adipocytes are modulated by lipolysis. **A,** Protein levels of IL1β in PC3 cells cultured alone or in Transwell with adipocytes in the absence or presence of lipolysis-inducing agent isoproterenol; representative blot is shown; **B,** IL1β densitometry normalized to β-actin; data represent the mean from 3 experiments; **C,** *IL1β* gene expression in PC3 cells upon treatment with isoproterenol; **D,** Protein levels of IL1β in PC3 cells cultured alone or in Transwell with adipocytes in the absence or presence of lipolysis-inducing agent Forskolin; representative blot is shown; **E,** IL1β densitometry normalized to tubulin; data represent the mean from three experiments; **F,** *IL1β* gene expression in PC3 cells upon treatment with Forskolin; **G,** *IL1β* gene expression in PC3 cells grown in Transwell cocultures with adipocytes in the absence or presence of 5 μmol/L inhibitor of hormone-sensitive lipase BAY59-9435 (BAY). **H,** *COX-2* mRNA levels in marrow adipocytes cultured alone or in Transwell with PC3 cells in the absence or presence of Forskolin; three individual experiments are shown. **I,** *COX-2* mRNA levels in marrow adipocytes grown in Transwell with PC3 cells and in the absence or presence of 5 μmol/L BAY. **J,** Gene expression of *HSL* and *ATGL* and free glycerol release (**K**) by adipocytes upon treatment with recombinant IL1β. *, $P < 0.05$; **, $P < 0.01$; ***, $P < 0.001$.

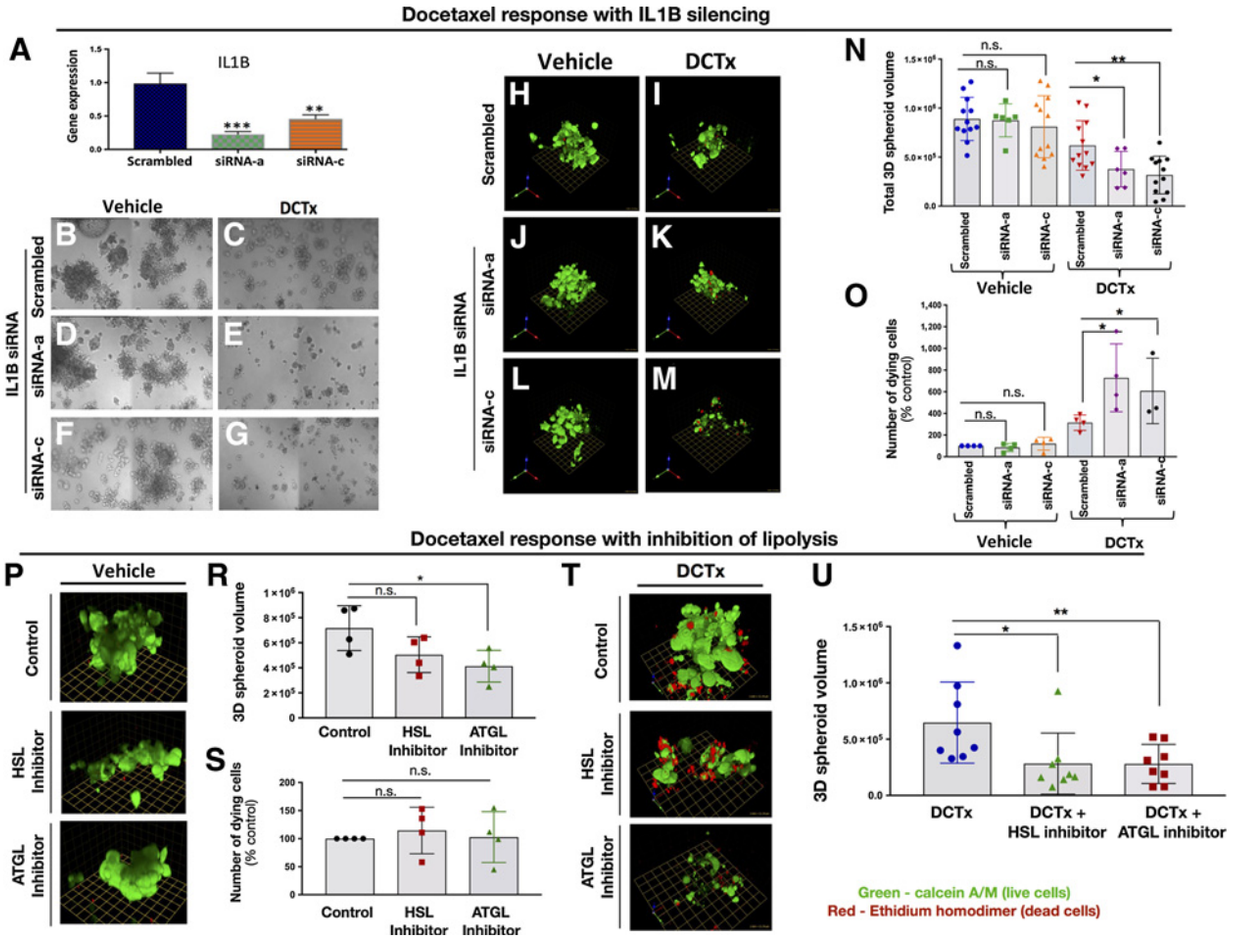

Figure 5.

IL1β silencing and inhibition of lipolysis sensitize ARCaP(M) spheroids to docetaxel treatment. **A,** *IL1β* mRNA levels in ARCaP(M) cells upon treatment with two nonoverlapping siRNAs. **B–G,** DIC tile images of 3D ARCaP(M) spheroids treated with scrambled control or IL1β siRNA A and C and grown in the absence (**B, D, F**) or presence **(C, E, G)** of 10 nmol/L DCTx. IL1β siRNA A and C have a visibly significant effect on spheroid size in the presence of DCTx. **H–M,** Live/Dead assay of control and IL1β silenced 3D cultures treated with vehicle (**H, J, L**) or 10 nmol/L DCTx (**I, K, M**). Green: Calcein AM–positive live cells; red: ethidium homodimer–positive dead cells; **N,** Quantification of spheroid volume in ARCaP(M) cells treated with scrambled control or IL1β siRNA in the absence or presence of DCTx **O,** Quantification of ethidium–positive (dead) cells/total spheroid volume shown as percent control; **P,** 3D images from Live/Dead assay on 3D cultures of ARCaP (M) cells grown in culture with adipocytes and exposed to HSL and ATGL inhibitors; **R,** Quantification of spheroid volume upon treatment with HSL inhibitor BAY59-9435 and ATGL inhibitor, Atglistatin; **S,** Quantification of ethidium–positive (dead) cells/total spheroid volume shown as percent control; **T,** 3D images from Live/Dead assay on 3D cultures of ARCaP(M) cells grown in culture with adipocytes and exposed to 10 nmol/L DCTx in the absence or presence of HSL and ATGL inhibitors; **U,** Quantification of total 3D spheroid volume in response to treatment. *, $P < 0.05$; **, $P < 0.01$; ***, $P < 0.001$.

presence of adipocytes (Fig. 1) can be overcome by reducing the levels of IL1β. Indeed, siRNA-mediated knockdown of IL1β in ARCaP(M) cells with two nonoverlapping siRNAs (Fig. 5A) reduced the size of tumor spheroids exposed to the DCTx treatment (Fig. 5B–G). Further examination by Live/Dead assay (Fig. 5H–M) confirmed reduced spheroid size (Fig. 5N) and revealed an augmented number of cells dying in response to DCTx upon IL1β knockdown (Fig. 5O). Because adipocyte-mediated IL1β expression in tumor cells appears to be modulated by lipolysis, we next determined whether sensitivity to DCTx treatment can be further increased by using inhibitors of lipases HSL and ATGL. Under 2D conditions, HSL and ATGL inhibitors had minimal effects on tumor cell proliferation and viability. Cellular DNA concentrations in lysates were 106.9% ± 3.4% of vehicle control for BAY59-9435 and 108.4% ± 5.7% for Atglistatin-treated cells in the absence of adipocytes. In Transwell coculture with adipocytes, DNA concentrations were 95.5% ± 3.1% of vehicle control for BAY59-9435 and 84.1% ± 6.4% for Atglistatin. In 3D assays, in the presence of adipocytes (Fig. 5P), however, the volume of ARCaP(M) spheroids was moderately reduced in the presence of ATGL inhibitor, possibly due to a decreased supply of lipids for tumor growth (Fig. 5R). At the same time, neither HSL nor ATGL inhibitors alone showed any detectable toxicity toward the prostate cancer cells as demonstrated by the unchanged number of dying cells with treatment (Fig. 5S). On the other hand, the combined use of docetaxel and the inhibitors of lipolysis resulted in significant enhancement of sensitivity to DCTx as evident by significant reduction in spheroid volume, particularly in the presence of ATGL inhibitor (Fig. 5T and U). Severe disintegration of the spheroid upon combined DCTx/ATGL

inhibitor treatment and the resulting loss of the majority of ethidium homodimer-labeled red cells did not allow for accurate quantification of dying cells under these conditions.

Contribution of hypoxia to IL1β/COX-2/MCP-1 cross-talk

One known mechanism of IL1β regulation is via HIF1α-mediated transcription (33, 34). Indeed, our previous data have shown that adipocytes induce HIF1α signaling in prostate cancer cells (7). We also observe that, although IL1β levels induced by Transwell coculture are not further augmented under hypoxia (Fig. 6A), treatment with an inhibitor of HIF1α transcription (CAY10585) significantly reduces IL1β levels that were increased upon interaction with adipocytes (Fig. 6B–D). In addition, both hypoxia and Transwell coculture with tumor cells promote HIF1α signaling in adipocytes, as indicated by significantly augmented mRNA levels of *GLUT1* and *HIF1α* (Fig. 6E and F). This induction of a hypoxic phenotype parallels the robust increases in levels of *COX-2*, *mPGES*, and *MCP-1* (Fig. 6G; Supplementary Fig. S6E and S6F), suggesting the link between HIF1α signaling and inflammatory phenotype in adipocytes. Notably, *GLUT1* and *HIF1α* expression in adipocytes can be directly induced by exposure to recombinant IL1β (Fig. 6H and I) but not upon treatment with tumor cell–conditioned media (Fig. 6J and K). This indicates that the presence of both cell types in Transwell coculture might be needed for the effective activation of HIF1α signaling in adipocytes.

Adipocyte-supplied PGE_2 contributes to prosurvival signaling in tumor cells

Both hypoxia and PGE_2 signaling have been linked to prosurvival signaling in the tumor. Our previous studies have shown that exposure to adipocytes promotes clonogenic growth and significantly augments the expression of Survivin and Bcl-xl (23), which have been shown to be regulated by PGE_2 via EP receptor–

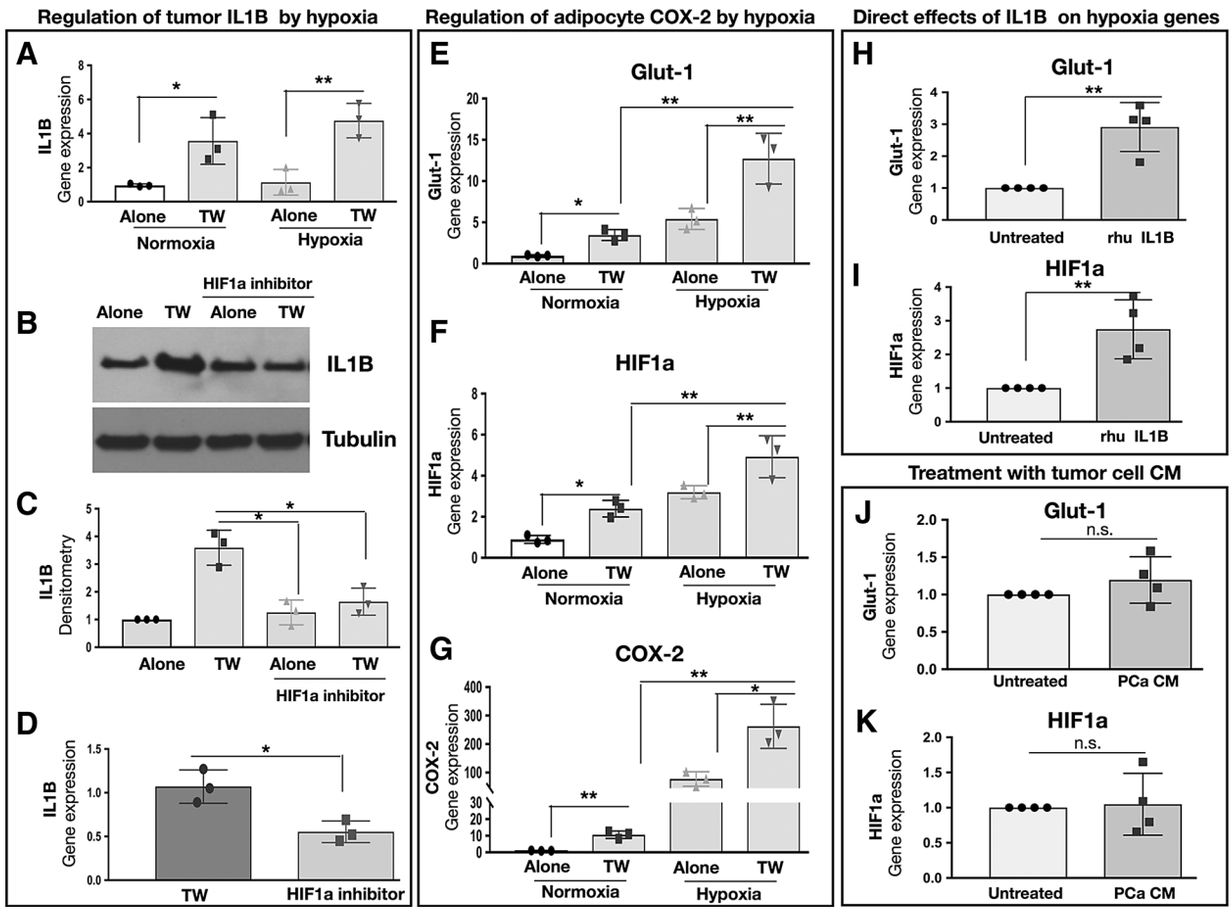

Figure 6.

COX-2 levels in adipocytes and IL1β levels in prostate cancer cells are sensitive to hypoxia. **A,** Gene expression of *IL1β* in PC3 cells cultured alone or in Transwell with adipocytes under normoxic or hypoxic conditions; **B,** IL1β protein levels in PC3 cells cultured alone or in Transwell and in the absence or presence of 5 μmol/L HIF1α inhibitor CAY10585; representative blot is shown; **C,** IL1β densitometry normalized to tubulin; data represent the mean ± SD from 3 separate experiments; **D,** *IL1β* gene expression in PC3 cells grown in Transwell cultures in the absence or presence of 5 μmol/L CAY10585. Gene expression of *GLUT1* (**E**), *HIF1α* (**F**), and *COX-2* (**G**) in bone marrow adipocytes cultured alone or in Transwell with PC3 cells under normoxic (21% O_2) or hypoxic (1% O_2) conditions. Data are shown as the mean of three biological replicate experiments. Gene expression of *GLUT1* (**H**) and *HIF1α* (**I**) of adipocytes upon treatment with recombinant IL1β. Gene expression of *GLUT1* (**J**) and *HIF1α* (**K**) of adipocytes upon treatment with media conditioned by prostate cancer cells; ± SD. *, $P < 0.05$; **, $P < 0.01$; n.s., not significant.

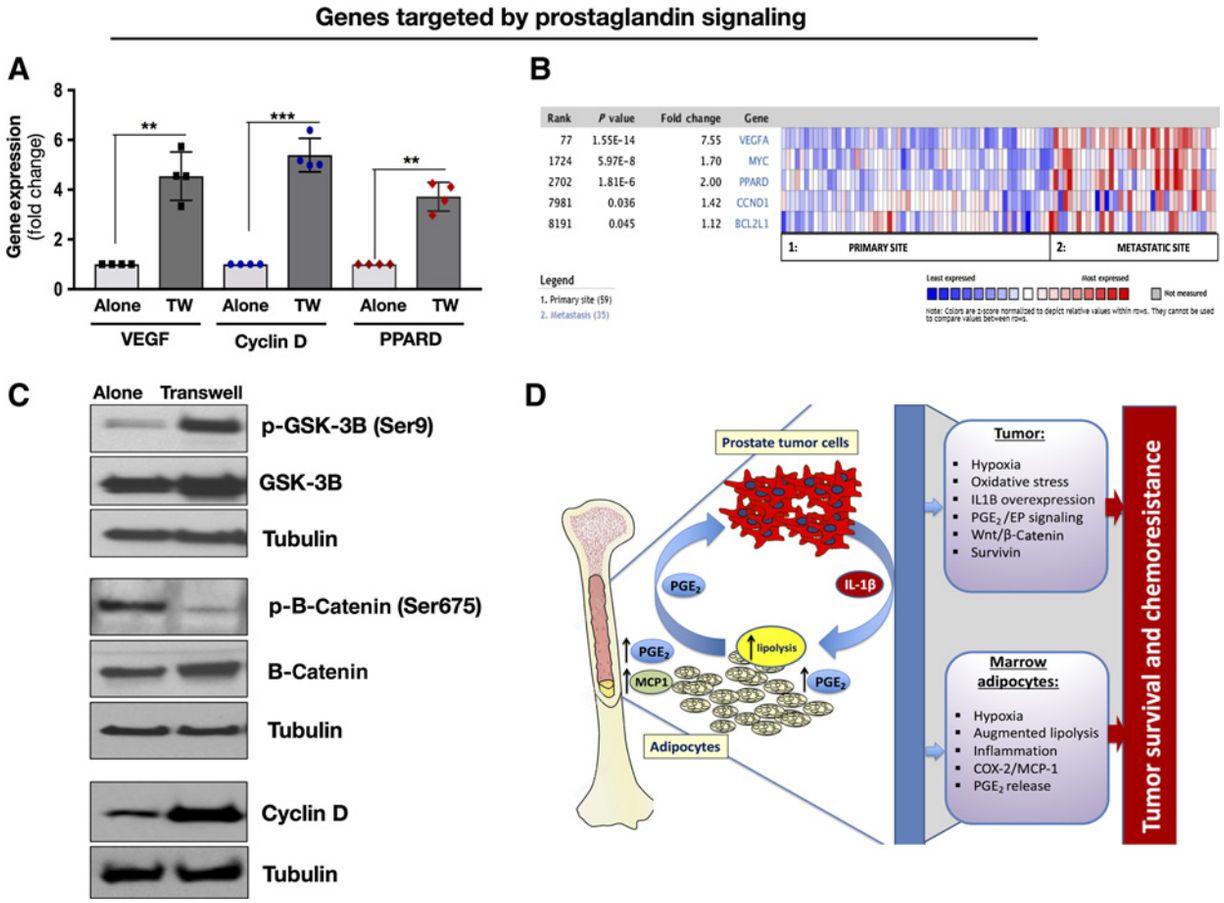

Figure 7.

Downstream targets of PGE_2 signaling are induced upon prostate cancer–marrow adipocyte cross-talk. **A,** Gene-expression analysis of *VEGF, Cyclin D,* and *PPARD* in PC3 cells cultured alone or in Transwell coculture with adipocytes; **B,** Oncomine gene analysis comparing the expression of prostaglandin/EP receptor target genes (*VEGF, MYC, PPARD*, and *CCND1*) in patient samples collected from metastatic or primary sites. Data were ordered by "overexpression," and the threshold was adjusted to $P < 1E-4$; fold change, 2 and gene rank, top 10%. **C,** Immunoblot analysis of p-GSK-3β (1:1,000), GSK-3β (1:1,000), p-β-catenin (1:1,000), β-catenin (1:1,000), and Cyclin D (1:1,000) proteins in PC3 cells grown alone or in Transwell with adipocytes. **D,** Proposed mechanism of adipocyte–tumor cell cross-talk involving the IL1β/COX-2/MCP-1 axis. Tumor cells stimulate adipocyte lipolysis. Lipolysis-mediated increase in IL1β and COX-2 levels and augmented production of PGE_2 lead to prosurvival effects on the tumor and therapy resistance.

mediated signaling (17, 35). Other targets of the PGE_2/EP axis, such as *VEGF, cyclin D*, and *PPARD,* are also highly induced upon Transwell culture with adipocytes (Fig. 7A). Notably, these gene targets are also augmented in metastatic versus primary prostate cancer tumors (Fig. 7B), indicating EP receptor signaling might be important in metastatic disease. Further evidence of adipocyte-mediated effects on prosurvival pathways in prostate cancer cells is the observed increase in phosphorylation of glycogen synthase kinase 3 (GSK-3β) at Ser9 and a coincident decrease in phosphorylation of β-catenin in prostate cancer cells grown in Transwell with adipocytes (Fig. 7C). This is in line with reduced kinase activity of GSK-3β and impeded targeting of β-catenin to the proteasome for degradation (36). Increased levels of cyclin D1 upon Transwell coculture further suggest that exposure to marrow adipocytes activates the Wnt/β-catenin pathway in tumor cells. Together, these results underscore the involvement of tumor-derived IL1β in regulating PGE_2 production by marrow adipocytes in collaborative effort to promote prosurvival signaling in tumor cells (Fig. 7D).

Discussion

Metastatic progression in the skeleton is a collaborative process between the tumor cells and bone microenvironment. As a major component of the adult bone marrow, adipocytes actively impact the metastatic niche via secretion of lipids, growth factors, adipokines, and inflammatory mediators (1, 2, 37). Inflammatory pathways, which under normal physiologic conditions protect and maintain normal bone homeostasis, are drastically altered under conditions of increased marrow adiposity (2). This is further complicated by the presence of metastatic tumor cells, capable of engaging marrow adipocytes in a cross-talk that ultimately supports tumor progression and survival. The present study focused on the adipocyte–tumor cell cross-talk involving tumor-supplied IL1β and adipocyte-derived COX-2 and MCP-1 in the context of DCTx response in prostate cancer. Our data revealed that IL1β expression in metastatic tumor cells is significantly induced by the exposure to marrow adipocytes *in vitro* and *in vivo*.

Reciprocally, adipocyte expression of COX-2 and MCP-1, and the consequent production of prostaglandins, are driven at least partially by tumor-supplied IL1β. Notably, this bidirectional adipocyte–tumor cell cross-talk appears to reduce sensitivity of prostate carcinoma cells to DCTx, a phenomenon muted by IL1β knockdown. Strikingly, inhibition of adipocyte lipolysis, a process that appears to regulate tumor IL1β and adipocyte COX-2/MCP-1 levels, leads to significant improvement in tumor cell response to DCTx. These findings suggest that activation of the inflammatory IL1β/COX-2/MCP-1 axis in the bone-tumor microenvironment might be a significant contributor to limited chemotherapy response in metastatic disease.

Traditionally, the main suppliers of IL1β in the tumor microenvironment are mononuclear phagocytes, fibroblasts, and lymphocytes, and the main functions of this cytokine are thought to involve the regulation of chemotaxis, cellular stress responses, and apoptosis (38). IL1β is mostly known as a component of an assembly complex of intracellular proteins termed the inflammasome, which is typically associated with immune cells (39). However, growing evidence begins to suggest this proinflammatory cytokine might play important functions in tumor cells. One potential mechanism of how cancer cell–supplied IL1β might be contributing to tumor progression is through a constitutively activated tumor-derived inflammasome as reported in late-stage melanoma (40). In prostate cancer specifically, several recent studies linked IL1β expression in prostate carcinoma cells with metastatic potential and successful colonization in bone (20, 22, 41). Recent studies also identified IL1β among cytokines whose circulating levels are increased in prostate cancer patients with progressive disease after DCTx treatment (42) and whose expression is augmented post-treatment, as compared with matched pretreatment tumor cells microdissected from biopsy samples (43). How tumor-supplied IL1β modulates bone-tumor microenvironment to evade therapy has not been previously studied.

Adipose tissue inflammation is tightly linked to adipocyte metabolism and inflammatory factors such as COX-2 and MCP-1, which have been shown to be sensitive to lipolytic stimulation (13). Our previous studies demonstrated that prostate cancer cells stimulate lipolysis in bone marrow adipocytes when grown under Transwell conditions (7). In the present study, we further show that IL1β expression by tumor cells and COX-2/MCP-1 levels in marrow adipocytes are sensitive to pharmacologic inducers and inhibitors of lipolysis, suggesting triglyceride hydrolysis might be a vital regulator of the inflammatory IL1β/COX-2/MCP-1 axis. More importantly, sensitivity of prostate cancer cells to DCTx treatment is significantly improved by IL1β knockdown and inhibition of lipolysis, linking triglyceride hydrolysis with IL1β-mediated prosurvival signaling in the tumor. IL1β has previously been reported to regulate lipid storage capacity in adipose tissue and to promote lipolysis by downregulating PPARγ in adipocytes (44). The mechanisms behind its direct contribution to marrow adipocyte lipolysis remain to be established.

The fact that adipocyte-derived COX-2 and MCP-1 appear to be regulated by tumor cell–derived IL1β has important implications in the context of metastatic progression. Both COX-2 and MCP-1 have been previously implicated in tumor-associated bone disease and reduced chemotherapy response via mechanisms attributed to their expression by the tumor cells (2, 45, 46). Importantly, prominent effects of host-derived MCP-1 on reduced DCTx response have been reported (47), underscoring the importance of bone-tumor microenvironment in chemotherapy resistance. Studies in prostate cancer suggested that COX-2 involvement in skeletal tumor growth is mediated via PGE_2 action on osteoblasts and activation of RANKL-mediated osteoclastogenesis and bone degradation (48). This is of importance as our lipidomics and gene-expression analyses indicate that adipocytes might be the predominant source of PGE_2 in adipocyte–tumor cell cocultures. Our data also show that adipocyte-supplied PGE_2 might be contributing to the prosurvival signaling in the tumor. We recognize that our study has limitations. Although we have utilized three independent *in vivo* models of marrow adiposity, all of which have shown that the production of PGE_2-producing enzymes in the host bone marrow is induced with tumor burden and correlates with adiposity, we cannot unequivocally link PGE_2 production in the bone-tumor microenvironment to marrow adipocytes. However, our data do collectively implicate adiposity-mediated IL1β/PGE_2 signaling in tumor-induced bone disease. Further investigations utilizing adipocytes isolated from control and tumor-bearing mice will deepen our understanding of this axis in metastatic disease.

The rate-limiting step in the production of IL1β is its transcription, and one of the candidate transcriptional regulators of IL1β, previously demonstrated in macrophages and astrocytes, is HIF1α (33, 34). Indeed, our previous studies have shown that HIF1α signaling is activated in prostate cancer upon adipocyte exposure, and it correlates with transformation to a glycolytic phenotype and enhanced lipid uptake by tumor cells (7). Studies presented herein further demonstrate that enhanced hypoxia signaling in both prostate cancer cells and the fat cells perpetuates the activation of the inflammatory IL1β/COX-2/MCP-1 axis in the adipocyte–tumor cell cross-talk. Previous studies in lung epithelial cells demonstrated that IL1β-mediated NFkB activation and subsequent increases in COX-2 expression and PGE_2 production lead to stabilization of HIF1α (49). Given our results demonstrating activation of NFkB in marrow adipocytes by tumor cell–supplied IL1β, it is plausible that this proinflammatory interplay contributes to stabilization of HIF1α and subsequent activation of prosurvival signaling. Our results demonstrating augmented expression of PGE_2/EP and Wnt/β-catenin target genes in tumor cells interacting with adipocytes further support this idea and call for further investigations.

Bone marrow niche is dynamic and complex, posing a major challenge to designing therapies that effectively target metastatic lesions within bone. Metastatic tumor cells engage specific components of the bone-tumor microenvironment to help them thrive in the marrow space and evade therapy. Stromal components of the bone were recently suggested to evoke chemoprotective effects on metastatic tumor cells via downregulation of latexin (50). Studies presented herein are the first to demonstrate that the interaction of prostate cancer cells with another component of bone marrow stroma, adipocytes, results in a functional cross-talk that involves tumor-supplied IL1β and adipocyte COX-2/MCP-1 pathways. Specifically, our data reveal for the first time that the hyperactivation of IL1β and COX-2/MCP-1 due to this bidirectional cross-talk promotes reduced sensitivity of tumor cells to docetaxel. Our studies also point to the hypoxic microenvironment within bone, as well as tumor-induced lipolysis in adipocytes, as the microenvironmental modulators of the IL1β/COX-2/MCP-1 axis that contribute to tumor aggressiveness

(Fig. 7D). Although COX-2 and MCP-1 have previously been suggested as targets for therapy, there has not been much success with blocking these pathways in metastatic disease. Results from this study underscore the significance of marrow adipose tissue inflammation in metastatic prostate cancer and demonstrate the need to study the mechanisms of its regulation during metastatic progression. Understanding the molecular mechanisms of hypoxia and lipolysis involvement in the regulation of the IL1β/COX-2/MCP-1 axis is critical toward identifying novel therapeutic approaches for cancers that thrive in adipocyte-rich bone marrow.

Disclosure of Potential Conflicts of Interest

No potential conflicts of interest were disclosed.

Authors' Contributions

Conception and design: M.K. Herroon, J.D. Diedrich, I. Podgorski
Development of methodology: M.K. Herroon, J.D. Diedrich, E. Rajagurubandara, I. Podgorski
Acquisition of data (provided animals, acquired and managed patients, provided facilities, etc.): M.K. Herroon, E. Rajagurubandara, C. Martin, K.R. Maddipati, E.I. Heath, I. Podgorski
Analysis and interpretation of data (e.g., statistical analysis, biostatistics, computational analysis): M.K. Herroon, J.D. Diedrich, E. Rajagurubandara, K.R. Maddipati, S. Kim, E.I. Heath, I. Podgorski
Writing, review, and/or revision of the manuscript: M.K. Herroon, J.D. Diedrich, K.R. Maddipati, E.I. Heath, J. Granneman, I. Podgorski
Administrative, technical, or material support (i.e., reporting or organizing data, constructing databases): M.K. Herroon, E. Rajagurubandara, I. Podgorski
Study supervision: I. Podgorski

Acknowledgments

We thank Dr. Kamiar Moin and the Microscopy, Imaging and Cytometry Resources Core (MICR) for assistance with confocal microscopy analyses. Grant support was provided by NIH/NCI 1 R01 CA181189 (I. Podgorski, PI), DOD W81XWH-14-1-0036 (I. Podgorski), NIH 5T32CA009531 (J.D. Diedrich), NIH/NCI 1F31CA203036 (J.D. Diedrich), Wayne State University Research Stimulus funds (I. Podgorski), and P30 CA 22453 (MICR).

The costs of publication of this article were defrayed in part by the payment of page charges. This article must therefore be hereby marked *advertisement* in accordance with 18 U.S.C. Section 1734 solely to indicate this fact.

Received May 22, 2019; revised August 19, 2019; accepted September 23, 2019; published first September 27, 2019.

References

1. Diedrich JD, Herroon MK, Rajagurubandara E, Podgorski I. The lipid side of bone marrow adipocytes: how tumor cells adapt and survive in bone. Curr Osteoporos Rep 2018;16:443–57.
2. Hardaway AL, Herroon MK, Rajagurubandara E, Podgorski I. Bone marrow fat: linking adipocyte-induced inflammation with skeletal metastases. Cancer Metastasis Rev 2014;33:527–43.
3. Reagan MR, Rosen CJ. Navigating the bone marrow niche: translational insights and cancer-driven dysfunction. Nat Rev Rheumatol 2016;12: 154–68.
4. Tannock IF, de Wit R, Berry WR, Horti J, Pluzanska A, Chi KN, et al. Docetaxel plus prednisone or mitoxantrone plus prednisone for advanced prostate cancer. N Engl J Med 2004;351:1502–12.
5. Nuhn P, De Bono JS, Fizazi K, Freedland SJ, Grilli M, Kantoff PW, et al. Update on systemic prostate cancer therapies: management of metastatic castration-resistant prostate cancer in the era of precision oncology. Eur Urol 2019;75:88–99.
6. Dirat B, Bochet L, Dabek M, Daviaud D, Dauvillier S, Majed B, et al. Cancer-associated adipocytes exhibit an activated phenotype and contribute to breast cancer invasion. Cancer Res 2011;71:2455–65.
7. Diedrich JD, Rajagurubandara E, Herroon MK, Mahapatra G, Huttemann M, Podgorski I. Bone marrow adipocytes promote the Warburg phenotype in metastatic prostate tumors via HIF-1alpha activation. Oncotarget 2016; 7:64854–77.
8. Shafat MS, Oellerich T, Mohr S, Robinson SD, Edwards DR, Marlein CR, et al. Leukemic blasts program bone marrow adipocytes to generate a protumoral microenvironment. Blood 2017;129:1320–32.
9. Balaban S, Shearer RF, Lee LS, van Geldermalsen M, Schreuder M, Shtein HC, et al. Adipocyte lipolysis links obesity to breast cancer growth: adipocyte-derived fatty acids drive breast cancer cell proliferation and migration. Cancer Metab 2017;5:1.
10. Nieman K, Kenny H, Penicka C, Ladanyi A, Buell-Gutbrod R, Zillhardt M, et al. Adipocytes promote ovarian cancer metastasis and provide energy for rapid tumor growth. Nat Med 2011;17:1498–503.
11. de Paula FJA, Rosen CJ. Structure and function of bone marrow adipocytes. Compr Physiol 2017;8:315–49.
12. Falank C, Fairfield H, Reagan MR. Signaling interplay between bone marrow adipose tissue and multiple myeloma cells. Front Endocrinol 2016;7:67.
13. Gartung A, Zhao J, Chen S, Mottillo E, VanHecke GC, Ahn YH, et al. Characterization of eicosanoids produced by adipocyte lipolysis: implication of cyclooxygenase-2 in adipose inflammation. J Biol Chem 2016; 291:16001–10.
14. Chan PC, Hsiao FC, Chang HM, Wabitsch M, Hsieh PS. Importance of adipocyte cyclooxygenase-2 and prostaglandin E2-prostaglandin E receptor 3 signaling in the development of obesity-induced adipose tissue inflammation and insulin resistance. FASEB J 2016;30:2282–97.
15. Mottillo EP, Shen XJ, Granneman JG. beta3-adrenergic receptor induction of adipocyte inflammation requires lipolytic activation of stress kinases p38 and JNK. Biochim Biophys Acta 2010;1801:1048–55.
16. Craig MJ, Loberg RD. CCL2 (monocyte chemoattractant protein-1) in cancer bone metastases. Cancer Metastasis Rev 2006;25:611–9.
17. Molina-Holgado E, Ortiz S, Molina-Holgado F, Guaza C. Induction of COX-2 and PGE(2) biosynthesis by IL-1beta is mediated by PKC and mitogen-activated protein kinases in murine astrocytes. Br J Pharmacol 2000;131:152–9.
18. Ozaki K, Hanazawa S, Takeshita A, Chen Y, Watanabe A, Nishida K, et al. Interleukin-1 beta and tumor necrosis factor-alpha stimulate synergistically the expression of monocyte chemoattractant protein-1 in fibroblastic cells derived from human periodontal ligament. Oral Microbiol Immunol 1996;11:109–14.
19. Vila-del Sol V, Fresno M. Involvement of TNF and NF-kappa B in the transcriptional control of cyclooxygenase-2 expression by IFN-gamma in macrophages. J Immunol 2005;174:2825–33.
20. Liu Q, Russell MR, Shahriari K, Jernigan DL, Lioni MI, Garcia FU, et al. Interleukin-1beta promotes skeletal colonization and progression of metastatic prostate cancer cells with neuroendocrine features. Cancer Res 2013; 73:3297–305.
21. Herroon MK, Rajagurubandara E, Hardaway AL, Powell K, Turchick A, Feldmann D, et al. Bone marrow adipocytes promote tumor growth in bone via FABP4-dependent mechanisms. Oncotarget 2013;4:2108–23.
22. Shahriari K, Shen F, Worrede-Mahdi A, Liu Q, Gong Y, Garcia FU, et al. Cooperation among heterogeneous prostate cancer cells in the bone metastatic niche. Oncogene 2017;36:2846–56.
23. Herroon MK, Rajagurubandara E, Diedrich JD, Heath EI, Podgorski I. Adipocyte-activated oxidative and ER stress pathways promote tumor survival in bone via upregulation of Heme Oxygenase 1 and Survivin. Sci Rep 2018;8:40.
24. Herroon MK, Diedrich JD, Podgorski I. New 3D-culture approaches to study interactions of bone marrow adipocytes with metastatic prostate cancer cells. Front Endocrinol 2016;7:84.
25. Maddipati KR, Zhou SL. Stability and analysis of eicosanoids and docosanoids in tissue culture media. Prostaglandins Other Lipid Mediat 2011; 94:59–72.

26. Nakanishi M, Rosenberg DW. Multifaceted roles of PGE2 in inflammation and cancer. Semin Immunopathol 2013;35:123–37.
27. Rosen CJ, Ackert-Bicknell C, Rodriguez JP, Pino AM. Marrow fat and the bone microenvironment: developmental, functional, and pathological implications. Crit Rev Eukaryot Gene Expr 2009;19:109–24.
28. Ackert-Bicknell CL, Shockley KR, Horton LG, Lecka-Czernik B, Churchill GA, Rosen CJ. Strain-specific effects of rosiglitazone on bone mass, body composition, and serum insulin-like growth factor-I. Endocrinology 2009; 150:1330–40.
29. Ali AA, Weinstein RS, Stewart SA, Parfitt AM, Manolagas SC, Jilka RL. Rosiglitazone causes bone loss in mice by suppressing osteoblast differentiation and bone formation. Endocrinology 2005;146:1226–35.
30. Reed MJ, Scribner KA. In-vivo and in-vitro models of type 2 diabetes in pharmaceutical drug discovery. Diabetes Obes Metab 1999;1:75–86.
31. Bing C. Is interleukin-1beta a culprit in macrophage-adipocyte crosstalk in obesity? Adipocyte 2015;4:149–52.
32. Liu W, Reinmuth N, Stoeltzing O, Parikh AA, Tellez C, Williams S, et al. Cyclooxygenase-2 is up-regulated by interleukin-1 beta in human colorectal cancer cells via multiple signaling pathways. Cancer Res 2003;63: 3632–6.
33. Zhang W, Petrovic JM, Callaghan D, Jones A, Cui H, Howlett C, et al. Evidence that hypoxia-inducible factor-1 (HIF-1) mediates transcriptional activation of interleukin-1beta (IL-1beta) in astrocyte cultures. J Neuroimmunol 2006;174:63–73.
34. Tannahill GM, Curtis AM, Adamik J, Palsson-McDermott EM, McGettrick AF, Goel G, et al. Succinate is an inflammatory signal that induces IL-1beta through HIF-1alpha. Nature 2013;496:238–42.
35. Greenhough A, Smartt HJ, Moore AE, Roberts HR, Williams AC, Paraskeva C, et al. The COX-2/PGE2 pathway: key roles in the hallmarks of cancer and adaptation to the tumour microenvironment. Carcinogenesis 2009;30: 377–86.
36. Wu D, Pan W. GSK3: a multifaceted kinase in Wnt signaling. Trends Biochem Sci 2010;35:161–8.
37. Veldhuis-Vlug AG, Rosen CJ. Clinical implications of bone marrow adiposity. J Intern Med 2018;283:121–39.
38. van de Veerdonk FL, Netea MG, Dinarello CA, Joosten LA. Inflammasome activation and IL-1beta and IL-18 processing during infection. Trends Immunol 2011;32:110–6.
39. Petrilli V. The multifaceted roles of inflammasome proteins in cancer. Curr Opin Oncol 2017;29:35–40.
40. Okamoto M, Liu W, Luo Y, Tanaka A, Cai X, Norris DA, et al. Constitutively active inflammasome in human melanoma cells mediating autoinflammation via caspase-1 processing and secretion of interleukin-1beta. J Biol Chem 2010;285:6477–88.
41. Schulze J, Weber K, Baranowsky A, Streichert T, Lange T, Spiro A, et al. p65-Dependent production of interleukin-1β by osteolytic prostate cancer cells causes an induction of chemokine expression in osteoblasts. Cancer Lett 2012;317:106–13.
42. Mahon KL, Lin HM, Castillo L, Lee BY, Lee-Ng M, Chatfield MD, et al. Cytokine profiling of docetaxel-resistant castration-resistant prostate cancer. Br J Cancer 2015;112:1340–8.
43. Huang CY, Beer TM, Higano CS, True LD, Vessella R, Lange PH, et al. Molecular alterations in prostate carcinomas that associate with in vivo exposure to chemotherapy: identification of a cytoprotective mechanism involving growth differentiation factor 15. Clin Cancer Res 2007;13: 5825–33.
44. Nov O, Shapiro H, Ovadia H, Tarnovscki T, Dvir I, Shemesh E, et al. Interleukin-1beta regulates fat-liver crosstalk in obesity by auto-paracrine modulation of adipose tissue inflammation and expandability. PLoS One 2013;8:e53626.
45. Qian DZ, Rademacher BL, Pittsenbarger J, Huang CY, Myrthue A, Higano CS, et al. CCL2 is induced by chemotherapy and protects prostate cancer cells from docetaxel-induced cytotoxicity. Prostate 2010;70:433–42.
46. Rozel S, Galban CJ, Nicolay K, Lee KC, Sud S, Neeley C, et al. Synergy between anti-CCL2 and docetaxel as determined by DW-MRI in a metastatic bone cancer model. J Cell Biochem 2009; 107:58–64.
47. Loberg RD, Ying C, Craig M, Day LL, Sargent E, Neeley C, et al. Targeting CCL2 with systemic delivery of neutralizing antibodies induces prostate cancer tumor regression in vivo. Cancer Res 2007;67:9417–24.
48. Takahashi T, Uehara H, Bando Y, Izumi K. Soluble EP2 neutralizes prostaglandin E2-induced cell signaling and inhibits osteolytic tumor growth. Mol Cancer Ther 2008;7:2807–16.
49. Jung YJ, Isaacs JS, Lee S, Trepel J, Neckers L. IL-1beta-mediated up-regulation of HIF-1alpha via an NFkappaB/COX-2 pathway identifies HIF-1 as a critical link between inflammation and oncogenesis. FASEB J 2003;17:2115–7.
50. Zhang M, Osisami M, Dai J, Keller JM, Escara-Wilke J, Mizokami A, et al. Bone microenvironment changes in latexin expression promote chemoresistance. Mol Cancer Res 2017;15:457–66.